Two novel TSC2 mutations in renal epithelioid angiomyolipoma sensitive to everolimus

Tao Wang, Shunqiang Xie, Rongtuan Luo, Lianguo Shi, Peide Bai, Xuegang Wang, Rui Wan, Jiang Deng, Zhun Wu, Wei Li, Wen Xiao, Yongfeng Wang, Bin Chen, Kaiyan Zhang & Jinchun Xing

View supplementary material �

Published online: 10 Oct 2019.

Submit your article to this journal �

Article views: 68

View related articles �

View Crossmark data �

Taylor & Francis
Taylor & Francis Group

BEDSIDE-TO-BENCH REPORT

Check for updates

Two novel TSC2 mutations in renal epithelioid angiomyolipoma sensitive to everolimus

Tao Wang[a]*, Shunqiang Xie[a]*, Rongtuan Luo[a], Lianguo Shi[b], Peide Bai[a], Xuegang Wang[a], Rui Wan[a], Jiang Deng[a], Zhun Wu[a], Wei Li[a], Wen Xiao[a], Yongfeng Wang[a], Bin Chen[a], Kaiyan Zhang[a], and Jinchun Xing[a]

[a]The Key Laboratory of Urinary Tract Tumors and Calculi, Department of Urology Surgery, The First Affiliated Hospital, School of Medicine, Xiamen University, Xiamen, China; [b]Department of Pathology, The First Affiliated Hospital, School of Medicine, Xiamen University, Xiamen, China

ABSTRACT

People who suffers renal angiomyolipoma (AML) has a low quality of life. It is widely known that genetic factors including TSC2 mutation contribute to certain populations of renal AML-bearing patients. In this study, we are the first to identify novel TSC2 mutations in one Chinese renal epithelioid AML patient: c.2652C>A; c.2688G>A based on sequencing result from biopsy tissue. These two somatic mutations cause a translational stop of TSC2, which leads to mTORC1 activation. Given the fact that activation of mTORC1 ensures cell growth and survival, we applied its inhibitor, FDA-approved everolimus, to this woman. After months of treatment with everolimus, Computer-Tomography (CT) scan results showed that everolimus successfully reduced tumor growth and distal metastasis and achieved partial response (PR) to everolimu according to Response Evaluation Criteria in Solid Tumors (RECIST version 1.1). Further Blood Routine Examination results showed the concentration of red cell mass, hemoglobin, white blood cell (WBC), platelets and hematocrit (HCT) significantly returned to normal levels indicating patients with these two TSC2 mutations could be effectively treated by everolimus.

Introduction

With an approximate 1–2 percent incidence, angiomyolipoma (AML) is considered as a mesenchymal tumor frequently detected in the kidney consisting of smooth-muscle-like cells, adipocyte-like cells, and epithelioid cells.[1-3] Typically, AMLs can be classified into classic variant and epithelioid variant based on the percentage of epithelioid cells. Characterizations of classic variant include abnormally thick-walled vessels and sparse epithelioid cells (usually less than 10 percent).[4,5] However, the epithelioid variant always has more than 10 percent of epithelioid cells, which are distinguished by abundant eosinophilic and granular cytoplasm. In clinical, more attention has been paid on epithelial variant because it can undergo malignant transformation.

Approximate 20% of renal AMLs is associated with tuberous sclerosis complex (TSC), an autosomal dominant multisystem disorder caused by the mutation of either TSC1 or TSC2.[6,7] TSC2/TSC1 complex is one central regulator of mTORC1 signaling pathway.[8,9] TSC2 complexes with TSC1 to inhibit mTORC1 signaling via driving Rheb into GDP-bound state, which acts as GTPase to activate mTORC1 when it is in GTP-bound state.[10,11] In the response to environmental stresses such as nutrients, oxygen, DNA damage, and growth factors, mTORC1 signaling is activated and controls cell growth and survival.[12,13] In addition, mTORC1 is also implicated into cancer development due to its regulation on cell proliferation, angiogenesis, and metastasis.[14-16] Therefore, mTORC1 is an appealing therapeutic target in clinic.

Indeed, mTORC1 inhibitors such as deforolimus, everolimus and temsirolimus have been prevalently assessed in various cancers, alone or in combination with other targeted therapies or chemotherapies.[17,18] Importantly, everolimus and temsirolimus were recently approved by the FDA for the treatment of renal cell carcinoma.

Here, we report a rare case of epithelioid renal AML. Biopsy tissue sequencing revealed that the patient carried two Somatic TSC2 mutation. Both mutations result in a translational stop of TSC2, which leads to mTORC1 activation. For this reason, FDA-approved eveolimus was administrated to control tumor progression.

Materials and methods

Fresh clinical kidney tumor tissues were collected according to the ethical guidelines of the Declaration of Helsinki (1975) and the Institutional Medical Ethics Committee of Xiamen University. Pathological diagnosis of BCa was verified by at least two pathologists.

DNA extraction

Tumor genomic DNA was extracted from AML biopsy tissue using the QIAamp DNA Micro Kit (Cat#56304, Qiagen) to identify potential mutations. DNA concentration was measured using a Qubit fluorometer (Cat#Q33216, Invitrogen)

and the Qubit dsDNA HS (High Sensitivity) Assay Kit (Cat#Q32854, Invitrogen). Total DNA was analyzed by second-generation sequencing for 1021 cancer-related genes. The loci of mutation in TSC2 was further validated by first-generation sequencing.

Targeted capture and next-generation sequencing

The next-generation sequencing of the tumor DNA was performed by Geneplus–Beijing Institute (Beijing, China). Firstly, about 1 µg of DNA was sheared by an ultrasonoscope to generate DNA fragments about 250 bps in length followed by end repair, A tailing, and ligation to the Illumina-indexed adapters. Then, the fragments were subjected to prepare library constructions by using the IlluminaTruSeq DNA Library Preparation Kit according to Manufacturer's instruction. Target enrichment was performed with a custom SeqCap EZ Library (Roche NimbleGen, Madison, WI, USA). Capture hybridization was carried out according to the manufacturer's protocol. Capture probes were designed to cover coding sequences or hot exons of 1,021 genes frequently mutated in solid tumors as shown in Table S1.[19] DNA sequencing was carried out with the HiSeq 3000 Sequencing System (Illumina, San Diego, CA) with 2 × 100-bp paired-end reads. Targeted capture sequencing revealed a mean effective depth of coverage of 671 ×.

RT-PCR and first-generation sequencing

For the Sequencing verification of TSC2, the primer pairs (Forward: CAGTATGCCAGTGTGTTCGCC; Reverse: AGTGAGCACACCCAGACAGTG) were designed based on the genomic sequences from the NCBI (https://www.ncbi.nlm.nih.gov/). A 641 bp of TSC2 DNA fragment were PCR-amplified using genomic DNA prepared from AML biopsy tissue with Pyrobest DNA Polymerase (Cat#DR500A, TaKaRa). The resultant DNA fragments were subjected to first-generation sequencing.

Frozen section and H & E staining

Briefly, the dissected biopsy tissue was mounted in OCT embedding compound and frozen at −20 to −80°C. Then, 10 µm thick tissue sections were made using a cryostat. Thaw-mount the sections onto gelatin-coated histological slides, which were pre-coated with gelatin to enhance adhesion of the tissue. H & E staining was performed on the frozen sections using Hematoxylin and Eosin reagents.

Immunohistochemistry staining and TFE3 FISH analysis

Antigen retrieval was performed on the deparaffinized and rehydrated tissue sections by boiling them in a citrate buffer (pH 6.0) for 30 min. After cooled down, the sections were treated with a peroxidase blocking buffer for another 30 min. After incubation with the blocking buffer (5% normal goat serum in PBS) for 1 h at room temperature, the sections were blotted with primary antibodies: HMB45 (Cat#MA1-34759, Thermo Fisher), Melan A (Cat#MA5-15237, Thermo Fisher), α-Smooth Muscle Actin (α-SMA) (Cat#14-9760-82, Thermo Fisher), PAX-8 (Cat#RAB-0657, MXB Biotechnologies, Fuzhou, China), Pan-Cytokeratin (Cat#RAB-0050, MXB Biotechnologies) and TFE3 (Cat#PA5-54909, Thermo Fisher). Then, biotin-labeled secondary antibody was added for another 30 min, followed by 30 min streptavidin incubation and signals were determined by DAB staining. TFE3 FISH detection was performed according to the manufacturer's instructions as described.[20]

Western blot analysis

Tissues were lysed in an ice-cold RIPA lysis buffer. 40 µg protein were loaded for electrophoresis on 8% denaturing SDS-PAGE gels. After transferred to PVDF membrane, the blots were probed with the primary antibodies overnight at 4°C, followed by incubation with secondary antibodies at room temperature for 2 h. The following primary antibodies were used: mTOR (Cat#2983, Cell Signaling), TSC2 (Cat#3612, Cell Signaling) and GAPDH (Cat#5174, Cell Signaling).

Results

In September 2016, one 46-year-old woman with pain in abdomen was referred to Department of Urology Surgery, The First Affiliated Hospital of Xiamen University. Image from Computer-Tomography (CT) scan showed that a huge mass existed on the dorsolateral surface of the left kidney with uneven density, which was suspected to be renal carcinoma (data not shown). Then, this patient was undergone radical nephrectomy surgery on 27 September and the size of the tumor tissue is about 10 × 9.5 × 6 cm (Figure 1(a)). Subsequently, the tumor tissue was subjected to histological analysis. Unexpectedly, an examination of frozen section revealed that this woman had renal AML, with densely eosinophilic cytoplasm and large hyperchromatic nucleus under the microscope (Figure 1(b)). Additionally, immunochemical staining with associated antibodies showed that this woman currently suffered from renal epithelioid AML (data not shown). We checked the medical history, CT and skin examination results and excluded the possibility of mental deficiencies and sebaceous adenoma in this patient. Together these results showed that this patient suffered from renal epithelioid AML rather than Tuberous Sclerosis Complex. One year later at 17 December 2018, this patient went back to our hospital for check. Surprisingly, we found that her tumor invaded into peritoneal and pelvic area based on the result from CT scan (Figure 4(a)). A biopsy tissue was subjected to histological analysis. Consistent with previous examination, H & E staining results revealed that this woman had renal AML (Figure 1(b)). Additionally, immunochemical staining with associated antibodies showed that the isolated tissue was positive for Melan A, HMB45, and TFE3, which are specific biomarkers for renal epithelioid AML (Figure 1(c)). Recently, Maria S. Tretiakova et al. reported that Eosinophilic solid and cystic renal cell carcinoma (ESC-RCC) is morphologically similar to a subset of tuberous sclerosis complex (TSC)-associated tumors and can mimic renal epithelioid AML.[21] Their further immunostaining analysis showed that ESC-RCC was positive for CK20 and melanocytic markers Melan-A, Cathepsin-K or HMB45, as well as PAX-8, whereas pan-cytokeratin and SMA were negative.
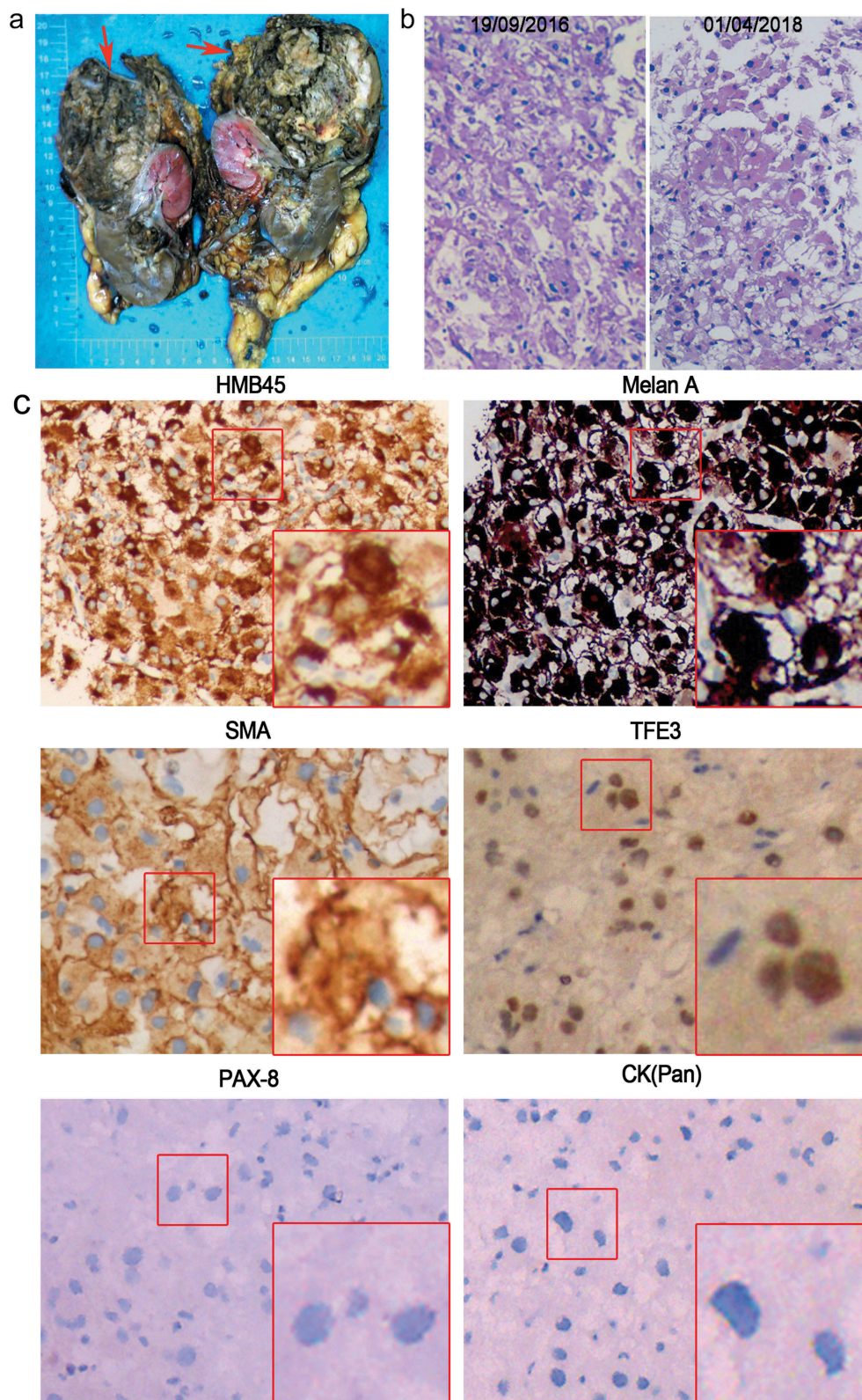
Figure 1. Identification of epithelioid AML in one Chinese woman. (a) Tumor mass after radical nephrectomy surgery. (b) H & E staining analysis of tumor tissues. (c-e) Immunohistochemistry analysis of tumor tissues. The patient's biopsy tumor tissues were stained with antibodies against HMB45, Melan A, SMA, TFE3, PAX-8, and CK (Pan).

Compared with all ESC-RCC, eAML cases were positive for either Melan-A or HMB45, most were positive for SMA (3/4), whereas all were negative for pan-cytokeratins AE1/AE3.[21] Consistent with their results, our further immunostaining analysis showed that SMA was positively expressed, whereas PAX-8 and pan-cytokeratin were negatively expressed in this case suggesting that this patient was eAML certainly. To further exclude the possibility of renal cell carcinoma associated with Xp11.2 translocation/TFE3 gene fusions, we performed TFE3-FISH analysis. TFE3-FISH result showed that
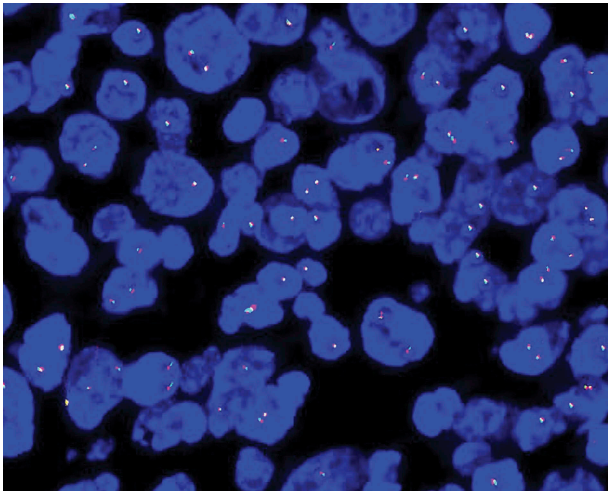
Figure 2. FISH analysis for TFE3 in tumor tissues. Statistical analysis showed that the percent of TFE3 fusion cells was less than 5% suggesting this patient was not Xp11.2 translocation renal cell carcinoma.

Table 1. TSC2 and LRP1B mutations analyzed by Next-generation DNA sequencing.

Gene	Base Alteration	Amino Acid Alteration	Region	Mutation Frequency
TSC2	c.2652 C > A	p. Y884*	Exon 24	7.0%
TSC2	c.2688 G > A	p. W896*	Exon 24	11.0%
LRP1B	c.6419 G > A	p.R2140K	Exon 40	7.6%

the rearrangements of TFE3 are rare and lower no more than 5% (Figure 2). Our targeted capture sequencing also conformed our FISH result (Table 1). Together, all these findings suggest that this patient currently suffered from kidney epithelioid AML.

AML is observed in 75% patients with tuberous sclerosis complex (TSC), which is caused by either TSC1 or TSC2 mutation. To identify which pathological mutation is responsible for this case, we screened a wide panel of 1021 cancer-associated genes using the biopsy tissue and found two somatic mutations in TSC2 and one somatic mutation in LRP1B, however, no germline mutation was detected (Table 1). One mutation in TSC2 is c.2652C>A, in which cytosine is replaced by adenine at position of 2652. Another one in TSC2 is c.2688G>A, in which a stop code was introduced at 896 amino acid residue. The stop code introduced at these two sites would lead to a truncated TSC2 transcript as indicated in Figure 3(a). Furthermore, RT-PCR was performed to amplify the TSC2 DNA fragment (Figure 3(b)). Indeed, sequencing analysis confirmed these two mutations (Figure 3(c,d)). On the other hand, Western blot results showed that the mutation at these two sites resulted in remarkably reduced expression levels of full-length TSC2 in AML tissue (Figure 3(e)). By contrast, mTOR was significantly up-regulated compared with control tissues (Figure 3(e)). Therefore, the translational premature of TSC2 causes a hyper-active mTORC1 signaling, which in turn promotes tumor cell growth and survival.
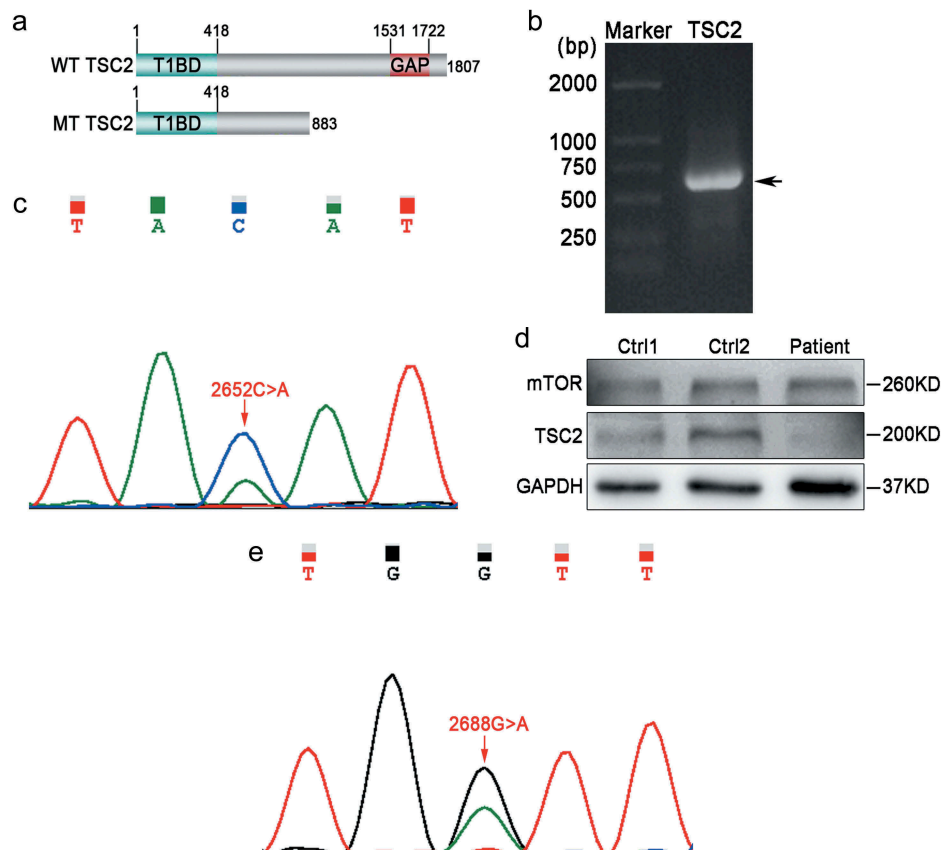
Figure 3. Mutations in TSC2 resulted in a truncated transcript and reduced protein levels. (a) Diagram of wild type (WT) and mutant TSC2 proteins, as predicted from cDNA and genomic sequencing in this AML patient. (b) RT-PCR showed the mutation region of TSC2 DNA in this patient. (c-d) First-generation sequencing to determine the loci of TSC2 mutations. (e) Western blotting showed that TSC2 expression was reduced in this patient, whereas mTOR was over expressed in tumor tissue. GAPDH served as a loading control.
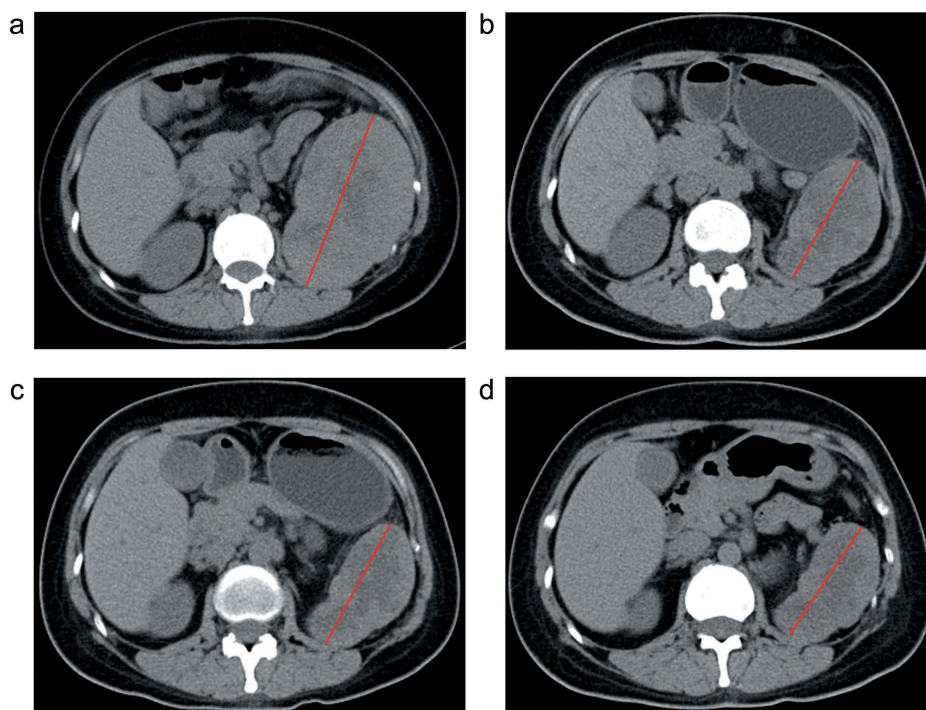
Figure 4. CT scan before and after everolimus uptake. (a) On 17 December 2018, CT scan showed that the size of the tumor was 12.74 × 8.47 cm. (b) After 1 month of everolimus uptake on 5 February 2018, CT scan showed that the size of the tumor was 9.46 × 5.12 cm. (c) After 2 months of everolimus uptake on 26 March 2018, CT scan showed that the size of the tumor was 8.91 × 4.81 cm. (d) After 4 months of everolimus uptake on 21 May 2018, CT scan showed that the size of the tumor was 8.25 × 4.6 cm.

Everolimus was approved by FDA to treat renal cell carcinoma for its efficient inhibition of mTORC1 activity. We sought to explore whether everolimus could ameliorate the progression of this type of AML. This patient was taken everolimus on 2 January 2018 and was checked every month by CT scanning. The images showed that the tumor mass was significantly reduced after drug administration (Figure 4(a–d)). After 4 weeks of drug administration, the tumor size was significantly reduced from 12.74 × 8.47 cm to 9.46 × 5.12 cm (Figure 4(a,b)). The sum of longest diameters decreased by 30.3%. According to Response Evaluation Criteria in Solid Tumors (RECIST version 1.1),[22] the patient achieved a partial response (PR) to everolimus. Four months after drug administration, the tumor size was significantly reduced to 8.25 × 4.6 cm and the sum of longest diameters decreased by 38.6% (Figure 4(d)). In addition, we evaluated her blood cells before and after everolimus uptake. Interestingly, this patient with lower values of red cell mass (*10^{12}/L), Hemoglobin (g/L) and hematocrit (HCT) before drug administration significantly improved and turned to normal levels after everolimus uptake (Figure 5(a–c), Table 2). While white blood cells (*10^{12}/L) and Platelets (*10^{12}/L) also returned to normal levels from abnormal (Figure 5(d,e), Table 2). Other blood routine index such as mean corpuscular hemoglobin concentration (MCHC, g/L), reticulocyte (RET, %), immature reticulocyte fraction (IRF, %), high light scattering reticulocyte (HLR, %), lymphocyte (LY, %), basophil (BA, %), monocyte (MO, %) and eosinophil (EO, %) were also returned to normal value from abnormally levels (Table 2). Blood cell analysis suggested her health status significantly got improved. Collectively, all these data indicate that the epithelioid AML in this woman was resulted from gene mutation of TSC2 and was successfully controlled by administration of everolimus.

Discussion

Renal AMLs are tightly related with tuberous sclerosis complex TSC1/2.[1] Here, we identified two mutations (c2652C>A; c2688G>A) in TSC2 according to our biopsy sequencing result. To our knowledge, our report about TSC2 mutation is novel even though numerous mutations in TSC2 have been reported. These two mutations cause translational stop of TSC2, leading to super activation of mTORC1 signaling so that this AML was sensitive to everolimus treatment. Indeed, administration of everolimus into this woman evidently reduced the progression of renal AML with these two TSC2 mutations. Early reports have been identified TSC2 mutations in AMLs such as c.1593C>T, c.3094C>T, c.4968C>T, c.228C>T, c.4780C>T and so on.[23-26] These mutations either introduced an early termination code in TSC2 or caused conformational change of TSC2. Here, our identified mutations (c2652C>A; c2688G>A) in TSC2 led to its reduced expression, which in turn triggered mTORC1 activation via maintaining Rheb in GTP-bound stage. Indeed, this kidney AML patient was very sensitive to mTORC1 inhibitor, everolimus. Our report strengthens the role of TSC1/2 complex in the development of AML and highlights the importance of TSC2 mutation as diagnostic tool or prognostic marker for renal epithelioid AML.

Normal cells require multiple mutations before they progress into uncontrolled malignant cells.[27] Indeed, we found
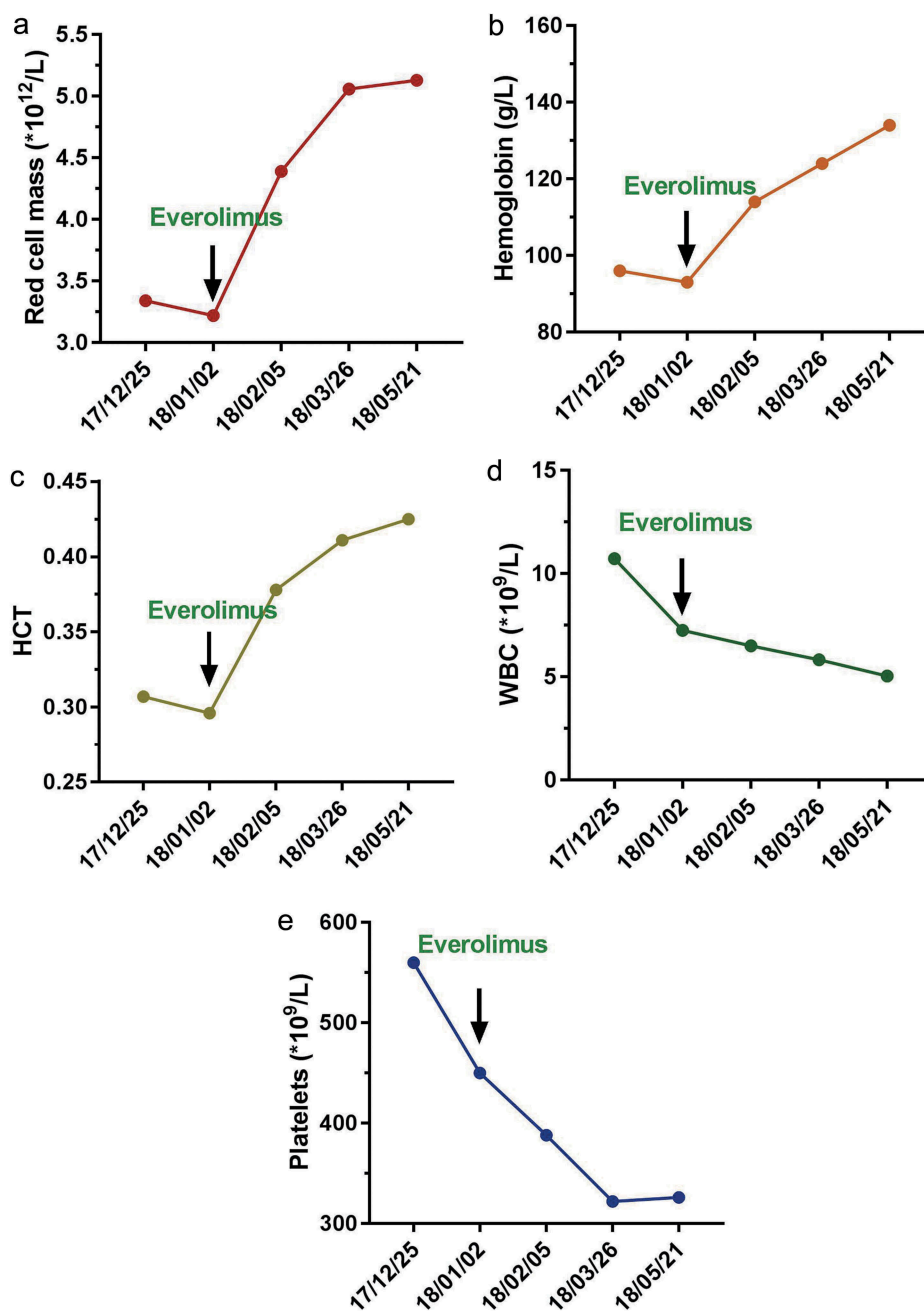
Figure 5. Symptoms of anemia, white blood cells and Platelets were significantly improved after everolimus administration. (a) Red cell mass (*10^{12}/L) level increased and returned to normal level after everolimus uptake. (b) Hemoglobin (g/L) level increased and returned to normal level after everolimus uptake. (c) HCT level increased and returned to normal level after everolimus uptake. (d) white blood cells (*10^{12}/L) level decreased and returned to normal level after everolimus uptake. (e) Platelets (*10^{12}/L) level decreased and returned to normal level after everolimus uptake.

there was a mutation in LRP1B (c.6419G>A). LRP1B (low-density lipoprotein receptor-related protein 1B) encodes a surface lipoprotein, which plays a role in endocytosis by binding and internalizing ligands.[28,29] As a tumor suppressor, the mutations of LRP1B have been widely reported in various cancers including lung cancer, skin cancer, and stomach cancer.[29-31] However, AML with LRP1B mutation has not been reported previously. Our report may build rational to further develop LRP1B mutation as either diagnostic marker or therapeutic target for AML.

In conclusion, we are the first to describe two novel mutations of TSC2 in Chinese kidney AML-bearing patient (c2652C>A;

c2688G>A), leading to the activation of mTORC1 signaling. Our present findings have important implications for the elucidation of the pathogenic mechanisms underlying kidney AML. Clinically, it provides a basis for the treatment of kidney AML patients.

Disclosure of Potential Conflicts of Interest

The authors declare that there is no conflict of interest that could be perceived as prejudicing the impartiality of the research reported.

Table 2. Main hematologic values before and after everolimus administration.

Index	Normal	17/12/25	18/01/02	18/02/05	18/03/26	18/05/21
Red cell mass ($*10^{12}$/L)	3.5 – 5	3.34	3.22	4.39	5.06	5.13
Hemoglobin (g/L)	110 – 150	96	93	114	124	134
HCT	0.37–0.45	0.307	0.296	0.378	0.411	0.425
MCV (fL)	86 – 100	91.9	91.9	86.1	81.2	82.8
MCH (pg)	27 – 34	28.70	28.90	26.00	24.50	26.10
MCHC (g/L)	316 – 354	313.00	314.00	302.00	302.00	315.00
RDW (%)	11.5–14.5	13.40	13.70	12.70	13.80	18.60
RET (%)	0.5–2.0	2.67	2.75	1.16	1.09	1.30
RET ($*10^6$/μL)	0.02–0.10	0.089	0.089	0.051	0.055	0.067
IRF	1.6–10.5	21.5	26.2	13.4	14.4	9.1
HLR	0 – 1.7	8.7	13.1	2.5	2.3	1.5
NRBC (%)	0 – 0	0	0	0	0	0
NRBC ($*10^9$/L)	0 – 0	0	0	0	0	0
EPO (mIU/mL)	-	NA	NA	NA	NA	NA
WBC ($*10^9$/L)	4 – 10	10.73	7.26	6.51	5.83	5.04
NE (%)	40 – 75	42.40	36.60	49.50	43.90	60.50
LY (%)	20 – 50	16.60	20.90	30.00	26.80	23.40
MO (%)	3 – 10	6.90	10.20	6.60	10.60	11.50
EO (%)	0.4–8.0	33.00	31.10	12.10	17.00	3.80
BA (%)	0 – 1	1.10	1.20	1.80	1.70	0.80
NE ($*10^9$/L)	1.8–6.3	4.55	2.65	3.22	2.56	3.05
LY ($*10^9$/L)	1.1–3.2	1.78	1.52	1.95	1.56	1.18
MO ($*10^9$/L)	0.1–0.6	0.74	0.74	0.43	0.62	0.58
EO ($*10^9$/L)	0.02–0.52	3.54	2.26	0.79	0.99	0.19
BA ($*10^9$/L)	0 – 0.06	0.12	0.09	0.12	0.10	0.04
Platelets ($*10^9$/L)	100 – 300	560	450	388	322	326
PCT	0.11–0.39	0.43	0.40	0.37	0.31	0.29
MPV (fL)	7.66 – 13.26	9.00	9.00	9.60	9.80	8.90
PDW (%)	9 – 17	8.70	8.80	10.00	10.30	9.90

References

1. Folpe AL, Kwiatkowski DJ. Perivascular epithelioid cell neoplasms: pathology and pathogenesis. Hum Pathol. 2010;41:1–15. doi:10.1016/j.humpath.2009.05.011.
2. Fujii Y, Ajima J, Oka K, Tosaka A, Takehara Y. Benign renal tumors detected among healthy adults by abdominal ultrasonography. Eur Urol. 1995;27:124–127. doi:10.1159/000475142.
3. Bissler JJ, Kingswood JC. Renal angiomyolipomata. Kidney Int. 2004;66:924–934. doi:10.1111/j.1523-1755.2004.00838.x.
4. Belanger EC, Dhamanaskar PK, Mai KT. Epithelioid angiomyolipoma of the kidney mimicking renal sarcoma. Histopathology. 2005;47:433–435. doi:10.1111/j.1365-2559.2005.02134.x.
5. Cibas ES, Goss GA, Kulke MH, Demetri GD, Fletcher CD. Malignant epithelioid angiomyolipoma ('sarcoma ex angiomyolipoma') of the kidney: a case report and review of the literature. Am J Surg Pathol. 2001;25:121–126. doi:10.1097/00000478-200101000-00014.
6. Eble JN. Angiomyolipoma of kidney. Semin Diagn Pathol. 1998;15:21–40.
7. Rakowski SK, Winterkorn EB, Paul E, Steele DJ, Halpern EF, Thiele EA. Renal manifestations of tuberous sclerosis complex: incidence, prognosis, and predictive factors. Kidney Int. 2006;70:1777–1782. doi:10.1038/sj.ki.5001853.
8. Inoki K, Li Y, Zhu T, Wu J, Guan KL. TSC2 is phosphorylated and inhibited by Akt and suppresses mTOR signalling. Nat Cell Biol. 2002;4:648–657. doi:10.1038/ncb839.
9. Fingar DC, Blenis J. Target of rapamycin (TOR): an integrator of nutrient and growth factor signals and coordinator of cell growth and cell cycle progression. Oncogene. 2004;23:3151–3171. doi:10.1038/sj.onc.1207542.
10. Xiao GH, Shoarinejad F, Jin F, Golemis EA, Yeung RS. The tuberous sclerosis 2 gene product, tuberin, functions as a Rab5 GTPase activating protein (GAP) in modulating endocytosis. J Biol Chem. 1997;272:6097–6100. doi:10.1074/jbc.272.10.6097.
11. Wienecke R, Konig A, DeClue JE. Identification of tuberin, the tuberous sclerosis-2 product. Tuberin possesses specific Rap1GAP activity. J Biol Chem. 1995;270:16409–16414. doi:10.1074/jbc.270.27.16409.
12. Saxton RA, Sabatini DM. mTOR signaling in growth, metabolism, and disease. Cell. 2017;168:960–976. doi:10.1016/j.cell.2017.02.004.
13. Laplante M, Sabatini DM. mTOR signaling in growth control and disease. Cell. 2012;149:274–293. doi:10.1016/j.cell.2012.03.017.
14. Majumder PK, Febbo PG, Bikoff R, Berger R, Xue Q, McMahon LM, Manola J, Brugarolas J, McDonnell TJ, Golub TR, et al. mTOR inhibition reverses Akt-dependent prostate intraepithelial neoplasia through regulation of apoptotic and HIF-1-dependent pathways. Nat Med. 2004;10:594–601. doi:10.1038/nm1052.
15. Raez LE, Papadopoulos K, Ricart AD, Chiorean EG, Dipaola RS, Stein MN, Rocha Lima CM, Schlesselman JJ, Tolba K, Langmuir VK, et al. A phase I dose-escalation trial of 2-deoxy-D-glucose alone or combined with docetaxel in patients with advanced solid tumors. Cancer Chemother Pharmacol. 2013;71:523–530. doi:10.1007/s00280-012-2045-1.
16. Pusapati RV, Daemen A, Wilson C, Sandoval W, Gao M, Haley B, Baudy AR, Hatzivassiliou G, Evangelista M, Settleman J. mTORC1-dependent metabolic reprogramming underlies escape from glycolysis addiction in cancer cells. Cancer Cell. 2016;29:548–562. doi:10.1016/j.ccell.2016.02.018.
17. Xie J, Wang X, Proud CG. mTOR inhibitors in cancer therapy. F1000Research. 2016;5:2078. doi:10.12688/f1000research.
18. Faes S, Demartines N, Dormond O. Resistance to mTORC1 inhibitors in cancer therapy: from kinase mutations to intratumoral heterogeneity of kinase activity. Oxid Med Cell Longev. 2017;2017:1726078. doi:10.1155/2017/1726078.
19. Wang Y, Zhao C, Chang L, Jia R, Liu R, Zhang Y, Gao X, Li J, Chen R, Xia X, et al. Circulating tumor DNA analyses predict progressive disease and indicate trastuzumab-resistant mechanism in advanced gastric cancer. EBioMedicine. 2019;43:261–269. doi:10.1016/j.ebiom.2019.04.003.
20. Yang B, Duan H, Cao W, Guo Y, Liu Y, Sun L, Zhang J, Sun Y, Ma Y. Xp11 translocation renal cell carcinoma and clear cell renal cell carcinoma with TFE3 strong positive immunostaining: morphology, immunohistochemistry, and FISH analysis. Mod Pathol. 2019. doi:10.1038/s41379-019-0283-z.
21. Tretiakova MS. Eosinophilic solid and cystic renal cell carcinoma mimicking epithelioid angiomyolipoma: series of 4 primary tumors and 2 metastases. Hum Pathol. 2018;80:65–75. doi:10.1016/j.humpath.2018.05.023.
22. Eisenhauer EA, Therasse P, Bogaerts J, Schwartz LH, Sargent D, Ford R, Dancey J, Arbuck S, Gwyther S, Mooney M, et al. New response evaluation criteria in solid tumours: revised RECIST guideline (version 1.1). Eur J Cancer. 2009;45:228–247. doi:10.1016/j.ejca.2008.10.026.
23. Yang HM, Choi HJ, Hong DP, Joo SY, Lee NE, Song JY, Choi Y-L, Lee J, Choi D, Kim B, et al. The analysis of mutations and exon deletions at TSC2 gene in angiomyolipomas associated with tuberous sclerosis complex. Exp Mol Pathol. 2014;97:440–444. doi:10.1016/j.yexmp.2014.09.013.
24. Espinosa M, Roldan-Romero JM, Duran I, de Alava E, Apellaniz-Ruiz M, Cascon A, Garrigos C, Robledo M, Rodriguez-Antona C. Advanced sporadic renal epithelioid angiomyolipoma: case report of an extraordinary response to sirolimus linked to TSC2 mutation. BMC Cancer. 2018;18:561. doi:10.1186/s12885-018-4242-8.

25. Nadiri M, Raeisi M, Mousavi Aghdas SA. A novel mutation in TSC2 gene: A 34-year-old female with pulmonary lymphangioleiomyomatosis with concomitant hepatic lesions. Case Rep Pulmonol. 2018;2018:5928231. doi:10.1155/2018/5928231.

26. Li S, Zhang Y, Wei J, Zhang X. Clinical and genetic analysis of tuberous sclerosis complex-associated renal angiomyolipoma in Chinese pedigrees. Oncol Lett. 2017;14:7085–7090. doi:10.3892/ol.2017.7079.

27. Knudson AG Jr. Mutation and cancer: statistical study of retinoblastoma. Proc Natl Acad Sci U S A. 1971;68:820–823. doi:10.1073/pnas.68.4.820.

28. Liu CX, Li Y, Obermoeller-McCormick LM, Schwartz AL, Bu G. The putative tumor suppressor LRP1B, a novel member of the low density lipoprotein (LDL) receptor family, exhibits both overlapping and distinct properties with the LDL receptor-related protein. J Biol Chem. 2001;276:28889–28896. doi:10.1074/jbc.M102727200.

29. Ding L, Getz G, Wheeler DA, Mardis ER, McLellan MD, Cibulskis K, Sougnez C, Greulich H, Muzny DM, Morgan MB. Somatic mutations affect key pathways in lung adenocarcinoma. Nature. 2008;455:1069–1075. doi:10.1038/nature07423.

30. Wang Z, Sun P, Gao C, Chen J, Li J, Chen Z, Xu M, Shao J, Zhang Y, Xie J. Down-regulation of LRP1B in colon cancer promoted the growth and migration of cancer cells. Exp Cell Res. 2017;357:1–8. doi:10.1016/j.yexcr.2017.04.010.

31. Prazeres H, Torres J, Rodrigues F, Pinto M, Pastoriza MC, Gomes D, Cameselle-Teijeiro J, Vidal A, Martins TC, Sobrinho-Simões M, et al. Erratum: chromosomal, epigenetic and microRNA-mediated inactivation of LRP1B, a modulator of the extracellular environment of thyroid cancer cells. Oncogene. 2017;36:146. doi:10.1038/onc.2016.143.